Since January 2020 Elsevier has created a COVID-19 resource centre with free information in English and Mandarin on the novel coronavirus COVID-19. The COVID-19 resource centre is hosted on Elsevier Connect, the company's public news and information website.

Biosensors and Bioelectronics 209 (2022) 114226

Contents lists available at ScienceDirect

Biosensors and Bioelectronics

journal homepage: www.elsevier.com/locate/bios

Protein sensors combining both on-and-off model for antibody homogeneous assay

Jie Li [a,1], Jin-Lan Wang [a,1], Wen-Lu Zhang [a,1], Zeng Tu [b], Xue-Fei Cai [a], Yu-Wei Wang [c,d], Chun-Yang Gan [a], Hai-Jun Deng [a], Jing Cui [a], Zhao-Che Shu [e], Quan-Xin Long [a], Juan Chen [a], Ni Tang [a], Xue Hu [e,**], Ai-Long Huang [a,***], Jie-Li Hu [a,*]

[a] Key Laboratory of Molecular Biology on Infectious Diseases, Ministry of Education, Chongqing Medical University, Chongqing, China
[b] Department of Immunology and Microbiology, Chongqing Medical University, Chongqing, China
[c] Department of Laboratory Medicine, Chongqing Hospital of Traditional Chinese Medicine, China
[d] Laboratory for Diagnosis and Treatment of Infectious Diseases Integrated Traditional Chinese and Western Medicine, Chongqing Hospital of Traditional Chinese Medicine, China
[e] The First Affiliated Hospital of Chongqing Medical University, Chongqing, 400016, China

ARTICLE INFO

Keywords:
Protein switch
Biosensor
NanoLuc
Antibody test
Homogeneous assay

ABSTRACT

Protein sensors based on allosteric enzymes responding to target binding with rapid changes in enzymatic activity are potential tools for homogeneous assays. However, a high signal-to-noise ratio (S/N) is difficult to achieve in their construction. A high S/N is critical to discriminate signals from the background, a phenomenon that might largely vary among serum samples from different individuals. Herein, based on the modularized luciferase NanoLuc, we designed a novel biosensor called NanoSwitch. This sensor allows direct detection of antibodies in 1 μl serum in 45 min without washing steps. In the detection of Flag and HA antibodies, NanoSwitches respond to antibodies with S/N ratios of 33-fold and 42-fold, respectively. Further, we constructed a NanoSwitch for detecting SARS-CoV-2-specific antibodies, which showed over 200-fold S/N in serum samples. High S/N was achieved by a new working model, combining the turn-off of the sensor with human serum albumin and turn-on with a specific antibody. Also, we constructed NanoSwitches for detecting antibodies against the core protein of hepatitis C virus (HCV) and gp41 of the human immunodeficiency virus (HIV). Interestingly, these sensors demonstrated a high S/N and good performance in the assays of clinical samples; this was partly attributed to the combination of off-and-on models. In summary, we provide a novel type of protein sensor and a working model that potentially guides new sensor design with better performance.

1. Introduction

Biosensors based on allosteric protein switches, fluorescent proteins, allosteric enzymes, and synthesized proteins have been extensively applied in detecting small molecules or biomacromolecules (Banala et al., 2013b; Frommer et al., 2009; Kim et al., 2021; Stein and Alexandrov, 2015; Villaverde, 2003). These sensors respond to the binding of targets via functional conformational and concomitant changes. Readouts reflecting these changes are used to quantify the concentration of targets. The close coupling of the binding and functional change provides protein switches with advantages of rapidity and convenience; repeated wash steps and liquid handing can be omitted, thereby achieving a homogeneous detection.

Allosteric enzymes can be engineered to protein switches responding to target binding with rapid changes in activity. Biosensors based on allosteric enzymes have been used to detect small molecules including calcium ions (Chen et al., 2013; Nagai et al., 2001), maltose (Guntas et al., 2005), rapamycin (Guo et al., 2019), and glucose (Joel et al., 2014); macromolecules including antibodies (Adamson et al., 2019; Banala et al., 2013a; Feliu et al., 2002; Ferrer-Miralles et al., 2001;

* Corresponding author.
** Corresponding author.
*** Corresponding author.
E-mail addresses: huxue@hospital.cqmu.edu.cn (X. Hu), ahuang@cqmu.edu.cn (A.-L. Huang), 102564@cqmu.edu.cn (J.-L. Hu).
[1] JL, JLW, and WLZ contributed equally to this work.

https://doi.org/10.1016/j.bios.2022.114226
Received 30 December 2021; Received in revised form 14 March 2022; Accepted 25 March 2022
Available online 31 March 2022

Geddie and Matsumura, 2007; Legendre et al., 1999), and proteins involved in apoptosis and inflammasome formation (Azad et al., 2014; Isazadeh et al., 2022; Torkzadeh-Mahani et al., 2012).

Among enzymes reconstructed to biosensors, luciferase NanoLuc (Nluc), engineered from a deep-sea shrimp by Hall and colleagues (Hall et al., 2012), has attracted significant research due to its small size and high luminescence efficacy. The Johnsson laboratory-developed bioluminescent sensor proteins (LUCIDs) using Nluc as a component for point-of-care monitoring of therapeutic drugs, metabolites, NAD+ and NADPH (Griss et al., 2014; Yu et al., 2018, 2019). Elsewhere, the Merkx lab developed a LUMABS platform, also based on Nluc to directly detect specific antibodies in blood plasma using a smartphone (Arts et al., 2016, 2017; van Rosmalen et al., 2018). Moreover, Nluc has been split into two parts complemented by themselves (LgBiT and HiBiT) or by interactions with other fused proteins (LgBiT and SmBiT) (Dixon et al., 2016). These modular pieces of NanoLuc provide a favorable basis for the design of novel protein switches. Several groups recently constructed split-Nluc-based biosensors to detect severe acute respiratory syndrome coronavirus 2 (SARS-CoV-2) antigens or specific antibodies (Elledge et al., 2021; Ni et al., 2021; Quijano-Rubio et al., 2021; Yao et al., 2021). A few of these biosensors demonstrated satisfactory performance in testing several cohorts of coronavirus disease 19 (COVID-19) patients (Elledge et al., 2021; Yao et al., 2021), indicating a potential clinical use of such biosensors.

One shortcoming in the construction of allosteric enzyme-based protein switches is the difficulty in achieving a high signal-to-noise ratio (S/N). In many cases, S/N constitutes a bottleneck for the clinical use of biosensors. The complex materials in serum plus variations among individuals require a relatively high S/N to discriminate signals from the background. A high S/N of the allosteric enzyme-based sensor is translated from a large difference in activity between the two states of the allosteric enzyme before and after target binding. Nonetheless, typical allosteric enzyme-based sensors hardly achieve a high S/N. For instance, sensors based on *E. coli* β-galactosidases showed S/N of less than 4-fold in the detection of antibodies (Feliu et al., 2002; Ferrer-Miralles et al., 2001). Besides, a modularized sensor based on TEM1-β-lactamase revealed an S/N of 7.6-fold in the detection of HA tag antibody. The highest S/N is from spLUC based on split Nluc, for which an over hundreds-fold increase in the signal upon antibody binding was noted (Elledge et al., 2021).

The present study designed a NanoSwitch, an alternative biosensor based on Nluc. This novel sensor allows direct detection of antibodies in 1 μl serum in 45 min without washing steps. A NanoSwitch for the detection of SARS-CoV-2-specific antibody revealed an S/N of over 200-fold in serum samples. Interestingly, this sensor works with a novel model, combining turn-off with human serum albumin and turn-on with specific antibodies. Moreover, we constructed NanoSwitches for detecting antibodies against HCV and HIV, which demonstrated satisfactory performance in the assays of clinical samples.

2. Materials and methods

2.1. Plasmids

Plasmids for gene expression in *E. coli* were constructed based on pET-28a (Novagen) using Golden Gate cloning (Engler et al., 2008). DNA sequences of the NanoSwitches for detecting the antibodies are listed in Supplementary Table 1. A flexible glycine-serine linker ((GGGGS)2) (Huston et al., 1988) was used to fuse the N-terminal epitope and the LgBiT in each NanoSwitch, and there is no linker between the LgBiT and the C-terminal epitope.

2.2. Serum samples

A total of 111 COVID-19 serum samples were obtained from 31 COVID-19 patients confirmed by real-time PCR. Then, sequential serum samples were collected from 15 of the 31 patients during hospitalization and after discharge. Non-COVID-19 serum samples were collected from 198 individuals chronically infected with the hepatitis B virus from the Second Affiliated Hospital of Chongqing Medical University before the pandemic. After collection, all the sera were heated to 56 °C for 30 min and stored at −80 °C before testing. For the detection of antibodies against the HCV core protein, 207 serum samples with HCV infection and 190 serum samples without HCV infection were collected from the First Affiliated Hospital of Chongqing Medical University. For the antibody against HIV gp41 protein assay, 93 serum samples with HIV infection and 92 serum samples without HIV infection were collected from the First Affiliated Hospital of Chongqing Medical University. The study was approved by the Ethics Commission of Chongqing Medical University (reference number: 2020003).

2.3. Pull-down experiment

Plasmids expressing NanoSwitch-1xFlag-3 were transfected into HEK293 cells. The cells were lysed using a lysis buffer (50 mM Tris-HCl; pH 7.4, 150 mM NaCl, 1% NP-40). The lysates were kept on ice for 20 min and centrifuged at 13,000 rpm for 15 min. Then, the supernatant was mixed with 2 μg of Flag antibody (Sigma, USA) and incubated for 1 h with shaking. Then, 40 μl of protein A magnetic beads (Bimake, China) was added and incubated with rotation at 4 °C for 1 h. The beads were washed 4 times using PBST, mixed with SDS sample buffer, and heated at 100 °C for 10 min to elute the proteins. After centrifugation at 13,000 rpm for 5 min, the supernatant was assayed by Western blot.

2.4. Western blot

Samples were boiled in SDS-PAGE sample loading buffer (Beyotime, China) at 100 °C for 10 min. Subsequently, the samples were separated by 12% sodium dodecyl sulfate-polyacrylamide gel electrophoresis (SDS-PAGE) then transferred to a polyvinylidene fluoride (PVDF) membrane (BioRad, USA). The membrane was blocked with 5% nonfat milk for 1 h, followed by overnight incubation with primary antibodies diluted in 5% nonfat milk. After washing, the membranes were revealed with goat anti-mouse IgG-Alexa Fluor 680 secondary antibody (LI-COR, USA) under an Odyssey CLx Infrared Imaging System (LI-COR, USA).

2.5. Expression of recombinant proteins

Genes for the recombinant proteins, including NanoSwitch-PG4-MC and NanoSwitch-1xFlag-2NM, were cloned into pET-28a. The plasmids were transformed into Rosetta (DE3) Competent Cells; the single clones were grown in LB medium supplemented with 50 μg/ml kanamycin. Protein expression was induced overnight at 16 °C and 180 rpm with 1 mM isopropyl-Beta-D-thiogalactopyranoside (IPTG) after the OD600 reached 0.6. Cells were harvested and resuspended in lysis buffer containing 20 mM phosphate (pH 7.5) and 500 mM NaCl. The supernatant of the lysate was loaded onto a prepacked Ni 2+ column. The column was thoroughly washed using 30 mM imidazole solution then eluted with 250 mM imidazole. The proteins were then dialyzed with cold 1x PBS (pH 7.5) at 4 °C. The final products were quantified and stored at −20 °C.

2.6. Detection of antibodies by NanoSwitches

Purified recombinant NanoSwitch proteins were incubated with the sera (1 μl for each reaction) or the antibodies in a protein reaction buffer containing 50 mM HEPES (pH 7.5), 3 mM EDTA, 150 mM NaCl, 0.005% (vol/vol) Tween-20, and 10 mM DTT. The reaction was conducted at 37 °C for 40 min, then the luminescence was detected using a Nano-Glo® Luciferase Assay System (Promega, USA) as per the manufacturer's instructions.

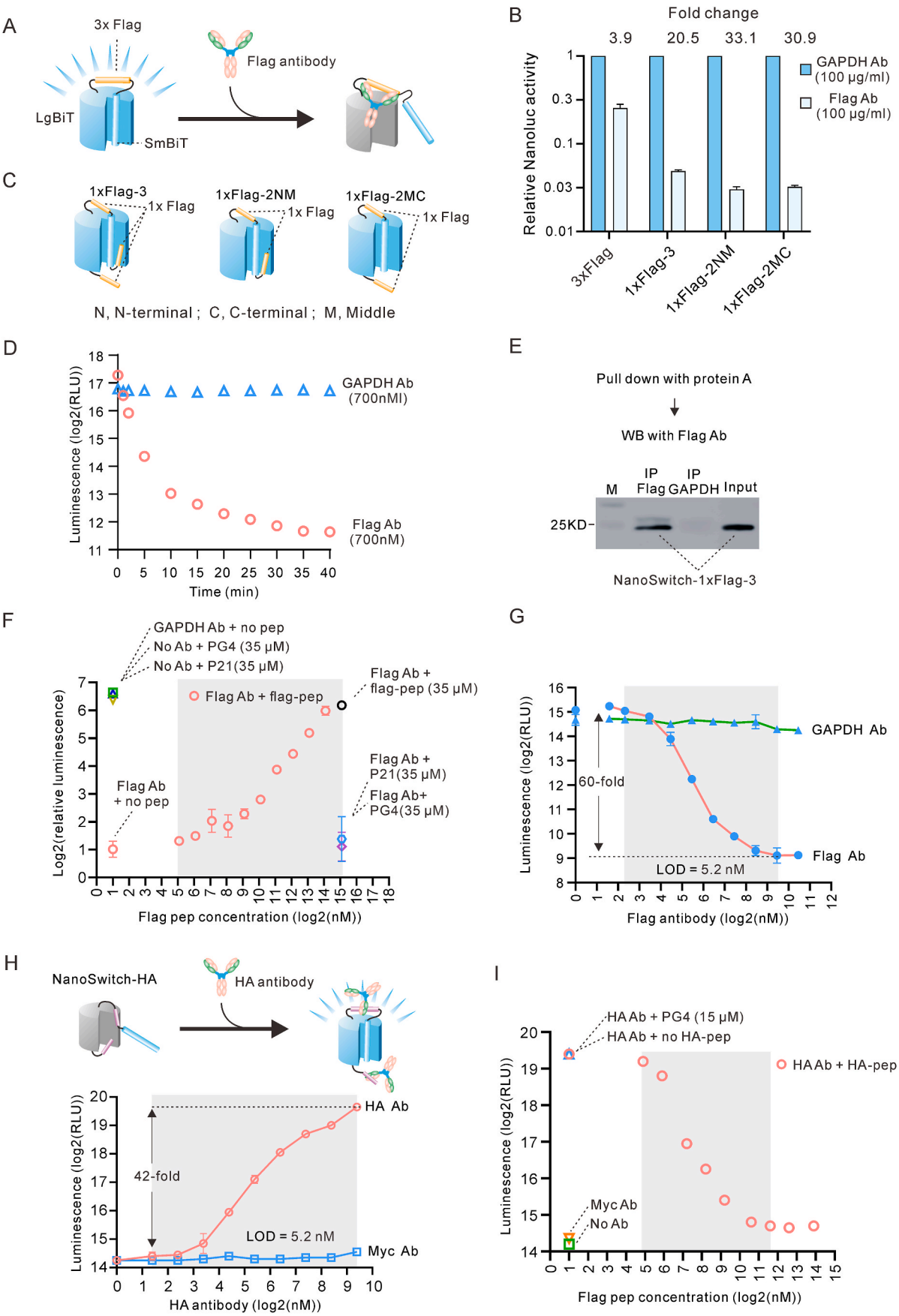

(caption on next page)

Fig. 1. Development of NanoSwitch for antibody detection
(A) Strategy for NanoSwitch construction. A 3xFlag tag was inserted between the LgBiT and SmBiT, and the binding of the antibody was supposed to turned off the switch; (**B**) Detection of Flag antibody by the NanoSwitches indicated in (**C**); (**C**) Three (1xFlag-3) or two 1xFlag tags (1xFlag-2) were placed at the N-terminus of the switches (stood for by the 'N'), the C-terminus of the switches ('C') and between the LgBiT and the SmBiT ('M') with the specified combinations. (**D**) Time course of the reaction between the NanoSwitch and Flag antibody; (**E**) Pull-down experiments of the NanoSwitch; (**F**) Competition experiments with Flag peptide; (**G**) The dynamic range of NanoSwitch-1xFlag-3; (**H**) Detection of HA antibody by NanoSwitch-HA. (**I**) Competition experiments with HA peptide. * Note: Protein reaction buffer (Materials and Methods) was used in Fig. 1 B, D, F–I, and the reaction was carried out at pH 7.5 and 37 °C.

2.7. Competition assay

For the competition assay of the NanoSwitches, peptides of Flag tag (DYKDDDDK), HA tag (YPYDVPDYA), PG4 (LQPELDSFKEELDKYFKNH TSPDVD), and P21 (PSKPSKRSFIEDLLFNKV) were synthesized (Sangon, Shanghai, China). Purified recombinant proteins were incubated with COVID-19 serum or antibodies in reaction systems containing 50 mM HEPES (pH 7.5), 3 mM EDTA, 150 mM NaCl, 0.005% (vol/vol) Tween-20, 10 mM DTT and different concentrations of synthetic peptides. The systems were conducted at 37 °C for 60 min, and luminescence was detected using a Nano-Glo® Luciferase Assay System (Promega, USA) following the manufacturer's instructions.

2.8. Purification of immunoglobulin from serum

Immunoglobulin was purified from serum samples with protein A/G magnetic beads (Bimake, China) according to the manufacturer's instructions. Briefly, 30 μl of serum was incubated with the protein A/G magnetic beads for 2 h at room temperature. After washing three times in washing buffer (50 mM Tris, 50 mM Nacl, 0.3% TritonX-100, pH 8.5), 20 μl of elution buffer (0.1 M Glycine, 0.3% TritonX-100, pH 3.1) was added and incubated at room temperature for 10 min. The mixture was then centrifuged for 10 min at 4 °C at 13000×*g*. The supernatant was transferred to a new tube and 1 μl of Neutralize buffer (1 M Tris, pH 8.0) was added to bring the pH to neutral.

2.9. Data analysis

Data were analyzed by Prism 8 (GraphPad, USA). Categorical variables were expressed as numbers (%) and compared by the χ^2 test or Fisher's exact test. To determine the cut-off values of the NanoSwitch tests for the antibodies from clinical samples, the luminescence value of each sample was input into Prism 8, and the receiver operating characteristic (ROC) curves, which were obtained by calculating the sensitivity and specificity of the tests at every possible cut-off point, were plotted according to the manufacturer's instructions. The cut-off value for each test was chosen so that the Youden-index (or maximal sensitivity + specificity) was maximal.

3. Results

3.1. Sensor design for detecting antibodies against Flag tag or HA tag

Splitting and evolution of Nluc resulted in two parts with low affinity, i.e., a large part (commercial name LgBiT, 156 amino acids) and a small part (commercial name SmBiT, 11 amino acids) (Dixon et al., 2016). These two parts have been extensively used to detect interactions between proteins of interest. In this work, these two parts were exploited to construct sensors for antibody detection. As shown in Fig. 1A, SmBiT was fused with the N-terminus of LgBiT, and an epitope (here 3xFlag tag) was inserted between SmBiT and LgBiT. We reasoned that low affinity between SmBiT and LgBiT (Kd = 190 μM) may influence their complementation by adjacently binding of Flag antibody and in turn affect the associated bioluminescence activity (Fig. 1A). The alteration in luminescence reflected the number of antibodies in the reaction system.

As expected, NanoSwitch-3xFlag responded to the Flag antibody, with a 3.9-fold inhibition of the luminescence signal (Fig. 1B). The sensor was optimized by distributing 1xFlag tags to different positions to increase the S/N (Fig. 1C). Consequently, NanoSwitch-1xFlag-2NM, with two 1xFlag tags located on the two sides of SmBiT, responded to the antibody with an average S/N of 33.1-fold (>60-fold in some repeats). The sensor completed the reaction with the Flag antibody at 37 °C for 40 min (Fig. 1D). Pull-down experiments revealed that the Flag antibody was bound to NanoSwitch-1xFlag-3 (Fig. 1E). The reaction was inhibited by the Flag peptide but not by two peptide controls in a dose-dependent manner (Fig. 1F), indicating the specificity of the reaction. The linear range of the detection was from 5 nM to 700 nM of the Flag antibody (Fig. 1G).

NanoSwitch for detecting HA tag antibody was constructed by inserting two 1xHA tags into the positions indicated in Fig. 1H. Interestingly, unlike the model of sensors for the Flag-tag antibody, this sensor responded to the HA-tag antibody but not to a control antibody with an increased signal (Fig. 1H); this indicates that the HA tags in the sensor might interfere with the association between SmBiT and LgBiT; the binding of HA antibody released this interference (Fig. 1H). The linear range of the detection was from 5 nM to 700 nM or more (Fig. 1H). Besides, adding the synthesized HA peptide to the system dose-dependently inhibited the signal induced by the HA antibody (Fig. 1I), hence confirming the specificity of the detection.

3.2. NanoSwitches for SARS-CoV-2 antibody detection

Inspired by the above results, we constructed NanoSwitches to detect antibodies against SARS-CoV-2. Two linear epitopes from the SARS-CoV-2 spike protein were first tested. One was used as a capture antigen (PG4), along with a recombinant nucleocapsid protein in an approved assay based on magnetic chemiluminescence enzyme immunoassay (MCLIA) (Long et al., 2020), while the other elicited neutralizing antibodies against SARS-CoV-2 (S21P2, hereafter abbreviated as P21) (Poh et al., 2020). One to three copies of the epitopes were incorporated into the sensor, and 4 serum samples from 4 COVID-19 patients and 2 controls were tested (Fig. 2A). As a consequence, the constructs containing 2 or 3 copies of both epitopes readily discriminated COVID-19 serum from the controls. Moreover, COVID-19 serum increased the luminescence of the NanoSwitches, and the highest increase in signal was 223-fold higher than that of the control serum (COVID-19 serum 1 detected by NanoSwitch-PG4-MC) (Fig. 2A). The increased luminescence of both NanoSwitch-PG4-MC and NanoSwitch-P21-MC in response to COVID-19 serum was inhibited by adding the synthesized peptides (Fig. 2B), indicating the specificity of the assay.

A total of 198 non-COVID-19 sera (collected before the pandemic) and 111 sera with positive SARS-CoV-2 IgG were tested to further evaluate the performance of NanoSwitch-PG4-MC (confirmed by MCLIA (Long et al., 2020)). As shown in Fig. 2C, this assay precisely discriminated most of the patient sera from non-COVID-19 sera. Receiver operating characteristic (ROC) curve analysis revealed an area under the ROC curve (AUC) of 0.9909 ($P < 0.0001$) (Fig. 2D). When the cutoff value was set to 1265 RLUs, a sensitivity of 97.3% and specificity of 97.0% were obtained (Fig. 2D). Antibody titers were calculated from this cutoff value, and the titer changes in 15 patients were compared with those obtained from the MCLIA. Fully consistent change models were observed in 13 of the 15 patients assayed by the two methods (Fig. 2E shows 6 representative results). Importantly, all of the IgG seroconversions (6/6) observed in the MCLIA were captured by

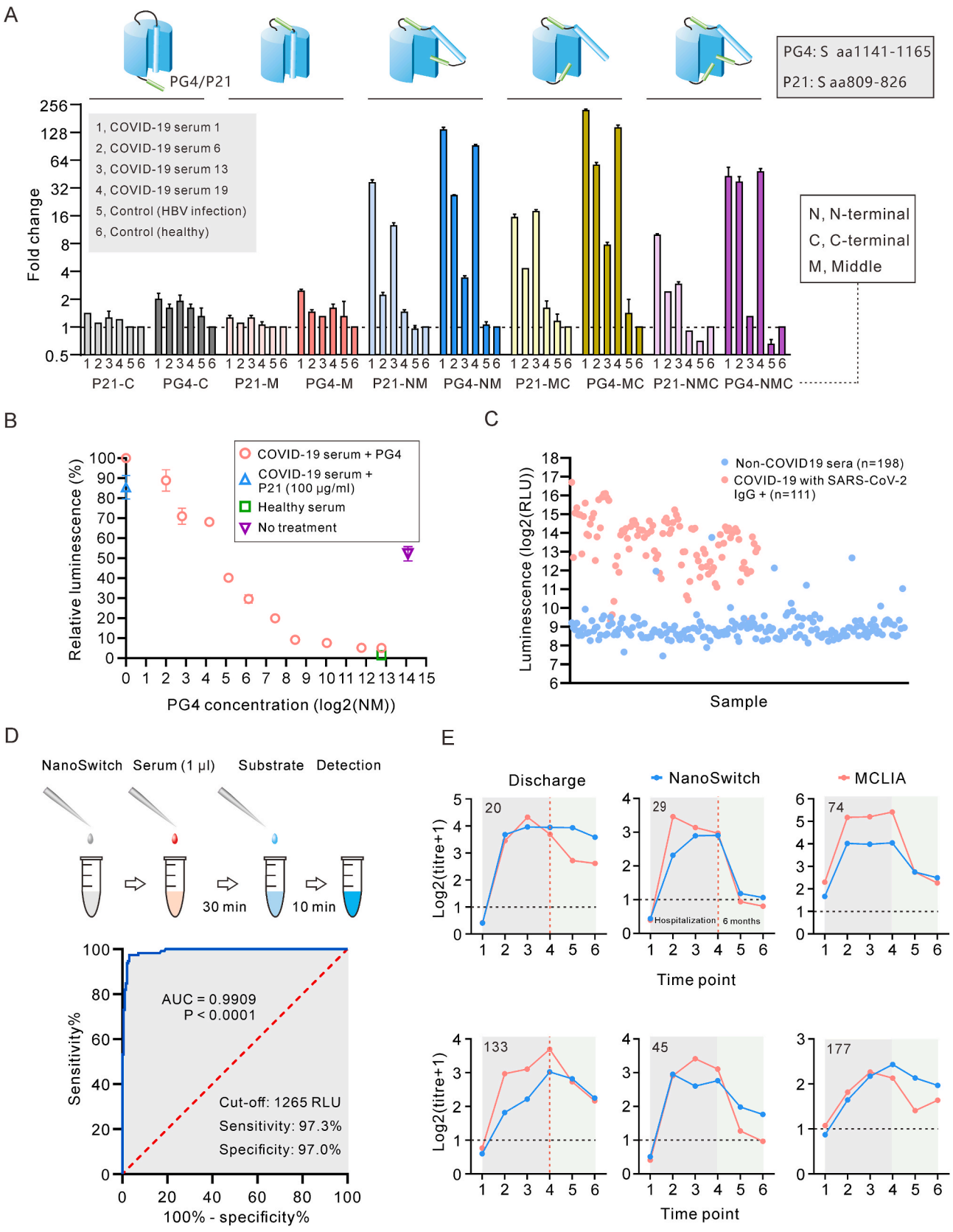

Fig. 2. Development of NanoSwitches for SARS-CoV-2 antibody detection
(**A**) Screening of the NanoSwitches; (**B**) Competition experiments with the synthesized peptides; (**C and D**) Assay of COVID-19 and non-COVID-19 sera; (**E**) Dynamic change in SARS-CoV-2 antibody titers in 6 patients determined by the two methods. * Note: Protein reaction buffer (Materials and Methods) was used in Fig. 2, and the reaction was carried out at pH 7.5 and 37 °C.

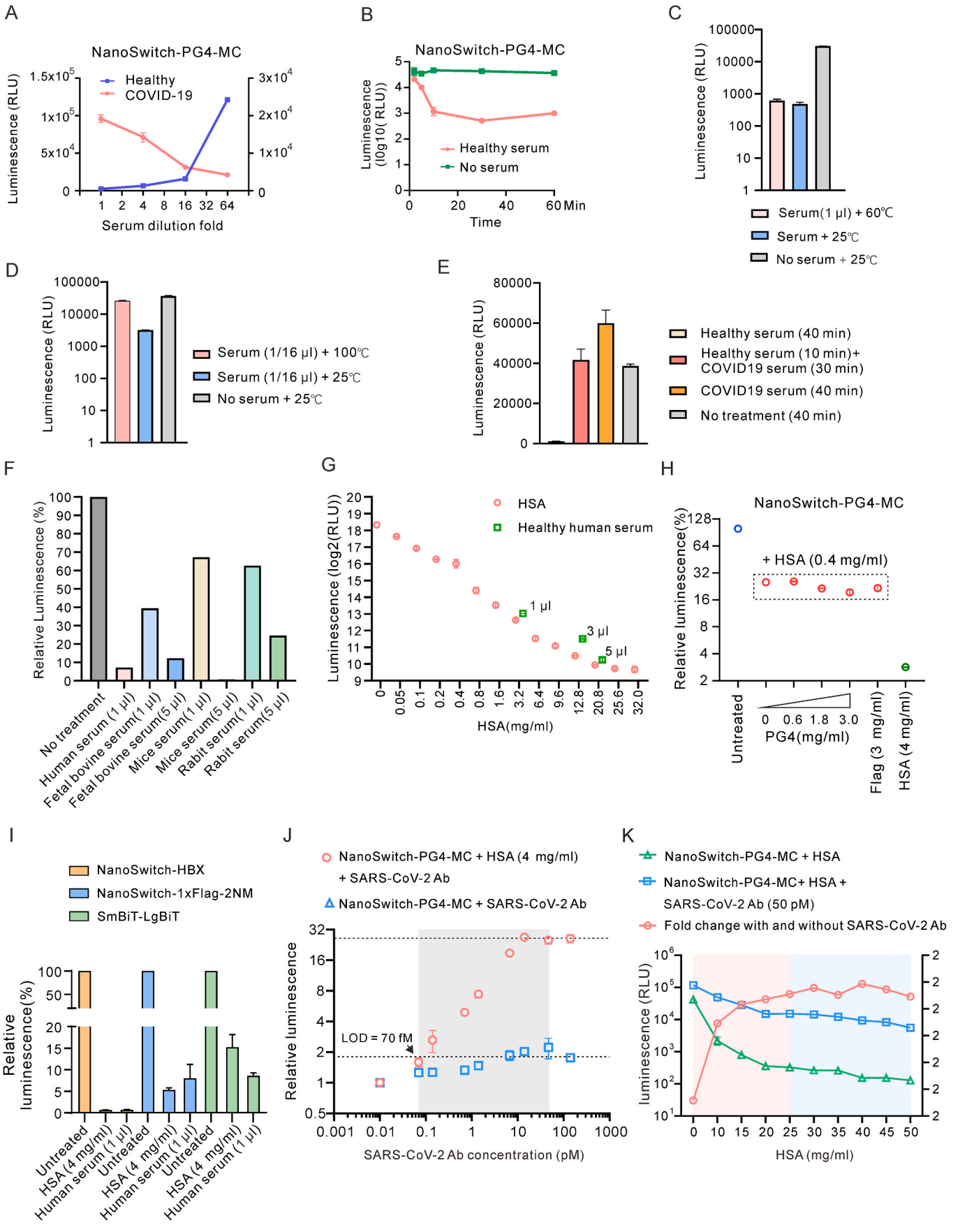

(caption on next page)

Fig. 3. NanoSwitch-PG4-MC working with a combination of OFF and ON models
(**A**) NanoSwitch-PG4-MC responded to COVID-19 and healthy sera differently; (**B**) Time course of the responses of NanoSwitch-PG4-MC to healthy serum; (**C** and **D**) Effects of temperature on the inhibition of the switch by healthy serum; (**E**) COVID-19 serum reversed the effects of healthy serum; (**F**) Several other sera also inhibited the switch to different extents; (**G**) HSA inhibited NanoSwitch-PG4-MC in a dose-dependent manner; (**H**) Peptide G4 did not inhibit the effect of HSA on the switch; (**I**) HSA and human serum inhibited another 2 NanoSwitches and SmBiT-LgBiT; (**J**) Responses of NanoSwitch-PG4-MC to multiclonal antibodies with or without has; (**K**) Responses of NanoSwitch-PG4-MC to the multiclonal antibodies in the presence of different concentrations of HSA. * Note: Protein reaction buffer (Materials and Methods) was used in Fig. 3 F–K, and the reaction was carried out at pH 7.5 and 37 °C.

NanoSwitch-PG4-MC. Only two patients showed different change models at 2-time points (Supplementary Fig. 1). This may be because antibodies against the nucleocapsid protein are detected by MCLIA (Long et al., 2020). These data indicate that the performance of NanoSwitch-PG4-MC is comparable to that of MCLIA in assays of clinical samples. Notably, the current method directly uses 1 μl serum for detection and needs only 3 steps, i.e., addition, incubation, and detection to complete the whole assay (Fig. 2D).

3.3. NanoSwitch-PG4-MC operates in an off-and-on model associated with human serum albumin

NanoSwitch-PG4-MC showed a higher S/N than that of NanoSwitch-P21-MC primarily because of a substance in the serum (healthy control) that significantly decreased the background of NanoSwitch-PG4-MC. Dilution of healthy serum increased the luminescent signal from NanoSwitch-PG4-MC, whereas dilution of COVID-19 serum decreased it (Fig. 3A); this indicates that the substance exerts an effect on the sensor opposite to the SARS-CoV-2 antibody. This substance acted in 10 min and was sensitive to heating at 100 °C (Fig. 3B, C, and D), suggesting that it might be a protein. COVID-19 serum reversed the inhibition caused by healthy serum (Fig. 3E), indicating that SARS-CoV-2 antibodies competed with the substance. Also, serum from rabbits, mice, and fetal bovines contained these substances but with lower effectivity (Fig. 3F). Thus, human serum albumin (HSA) was tested since it is the most abundant protein in serum prone to binding many molecules (Rabbani and Ahn, 2019). As expected, HSA dose-dependently inhibited NanoSwitch-PG4-MC (Fig. 3G). HSA at a concentration equivalent to that in human serum (4 mg/ml) turned off the switch to the same level as human serum (Fig. 3G). Nevertheless, adding the PG4 peptide did not inhibit the effect of HSA (Fig. 3H), indicating that the binding of HSA to NanoSwitch-PG4-MC is unlikely to be solely mediated by PG4 sequence. In line with this, 2 other NanoSwitches, i.e., NanoSwitch-1xFlag-2NM and NanoSwitch-HBX (containing a peptide from the X protein of hepatitis B virus), and even SmBiT-LgBiT were turned off by HSA and human serum to different extents (Fig. 3I). These results led to a hypothesis that HSA in serum turned off NanoSwitch-PG4-MC, whereas SARS-CoV-2 antibodies turned it on majorly by releasing HSA. To further test this hypothesis, NanoSwitch-PG4-MC was used to assay the rabbit multiclonal antibodies against a peptide (SARS-CoV-2 spike protein amino acids 994–1218) that covers the PG4 sequence (spike amino acids 1141–1165). These antibodies slightly (<2-fold) activated the switch when HSA was not present in the system (Fig. 3J). However, the addition of HSA improved the S/N to approximately 30-fold (Fig. 3J). Notably, 140 fM of the antibodies triggered a greater fold-change in the HSA system than that which was induced by 47 pM in the non-HSA system.

A concern with NanoSwitch-PG4-MC detection is that the variation of HSA in real samples might affect the testing results. To test the influence of HSA on the performance of NanoSwitch-PG4-MC, we added different amounts of HSA to the reaction system in the presence of the rabbit multiclonal antibodies (50 pM). As HSA concentrations increase in the range of 0–20 mg/ml, the luminescent signals from both the systems with and without the antibodies decrease abruptly, demonstrating the turn-off effect of HSA again (Fig. 3K). However, in the range of 20–50 mg/ml, this increasing trend flattens out, resulting in a relatively steady S/N level. These findings suggest that NanoSwitch-PG4-MC is unaffected by HSA in the range of 20–50 mg/ml. A prior study analyzed the variation of HSA in 1,079,193 serum samples from people of various ages. Almost all HSA concentrations are reported to be between 25 and 50 mg/ml (Weaving et al., 2016). Based on this information, we think HSA would have little impact on the performance of NanoSwitch-PG4-MC in practice.

3.4. NanoSwitch for detecting antibodies against the core protein of hepatitis C virus (HCV)

First, suitable peptides (epitopes) were screened to construct a NanoSwitch for detecting antibodies against the HCV core protein. The protein (191 amino acids in length) was dissected into 9 peptides with lengths of approximately 20 aa. These 9 peptides were incorporated into NanoSwitch at the positions indicated in Fig. 4A. A screening using serum samples from patients infected with HCV demonstrated that NanoSwitch peptide from the 21st to 40th amino acids (Fig. 4A) of the HCV core protein performed effectively among the 9 NanoSwitches (data not shown). This NanoSwitch (NanoSwitch-HCV-core) was expressed and purified from *E. coli* and used to detect antibodies against the HCV core protein in HCV-positive serum samples (n = 207) and controls (n = 190). The findings showed that when a cutoff value was set at 1387 RLU, the NanoSwitch-HCV-core discriminated positive and controlling samples with a sensitivity of 96.6% and a specificity of 96.8%.

Interestingly, we also noted that control serum samples reduced the NanoSwitch signal by approximately 10-fold. We purified the immunoglobulin from a serum sample with a positive HCV antibody using protein A affinity purification. The purified immunoglobulin turned 77-fold on the NanoSwitch-HCV-core without HSA (Fig. 4C). In contrast, adding control serum or HSA to the system augmented the response amplitude of the NanoSwitch-HCV-core to 96-fold and 161-fold, respectively. This indicates that a combination of off-and-on effects induced by HSA in serum improves the S/N of the NanoSwitch-HCV-core in detection. Furthermore, we tested how HSA affected the performance of NanoSwitch-HCV-core. HSA was introduced to the reaction system, with or without HCV antibodies isolated from a serum sample (not the sample used in Fig. 4C). As shown in Fig. 4D, with the increase of HSA, the S/Ns increased with increasing HSA in the range of 0–25 mg/ml, but this trend flattened in the range of 25–50 mg/ml, demonstrating that NanoSwitch-HCV-core is not sensitive to HSA in the range of 25–50 mg/ml.

3.5. NanoSwitch for detecting antibodies against gp41 of the human immunodeficiency virus (HIV)

Further, we constructed a NanoSwitch to detect antibodies against gp41 of HIV by incorporating a peptide (amino acids from 579th to 607th of gp41) into the indicated positions in Fig. 5A. This NanoSwitch (NanoSwitch-HIV-gp41) was expressed and purified from *E. coli* and used to detect serum samples from HIV-positive patients and controls. As shown in Fig. 5B, when the cutoff value was set at 3640 RLU, NanoSwitch-HIV-gp41 was positively discriminated from the control samples with a sensitivity of 86.2% and a specificity of 100%. Again, an approximately 20-fold decrease was observed in the NanoSwitch-HIV-gp41 signal after adding the control serum. To establish whether HSA caused this phenomenon, an immunoglobulin was purified from an HIV antibody-positive serum sample with magnetic beads coated with protein A. The purified immunoglobulin turned on NanoSwitch-HIV-gp41

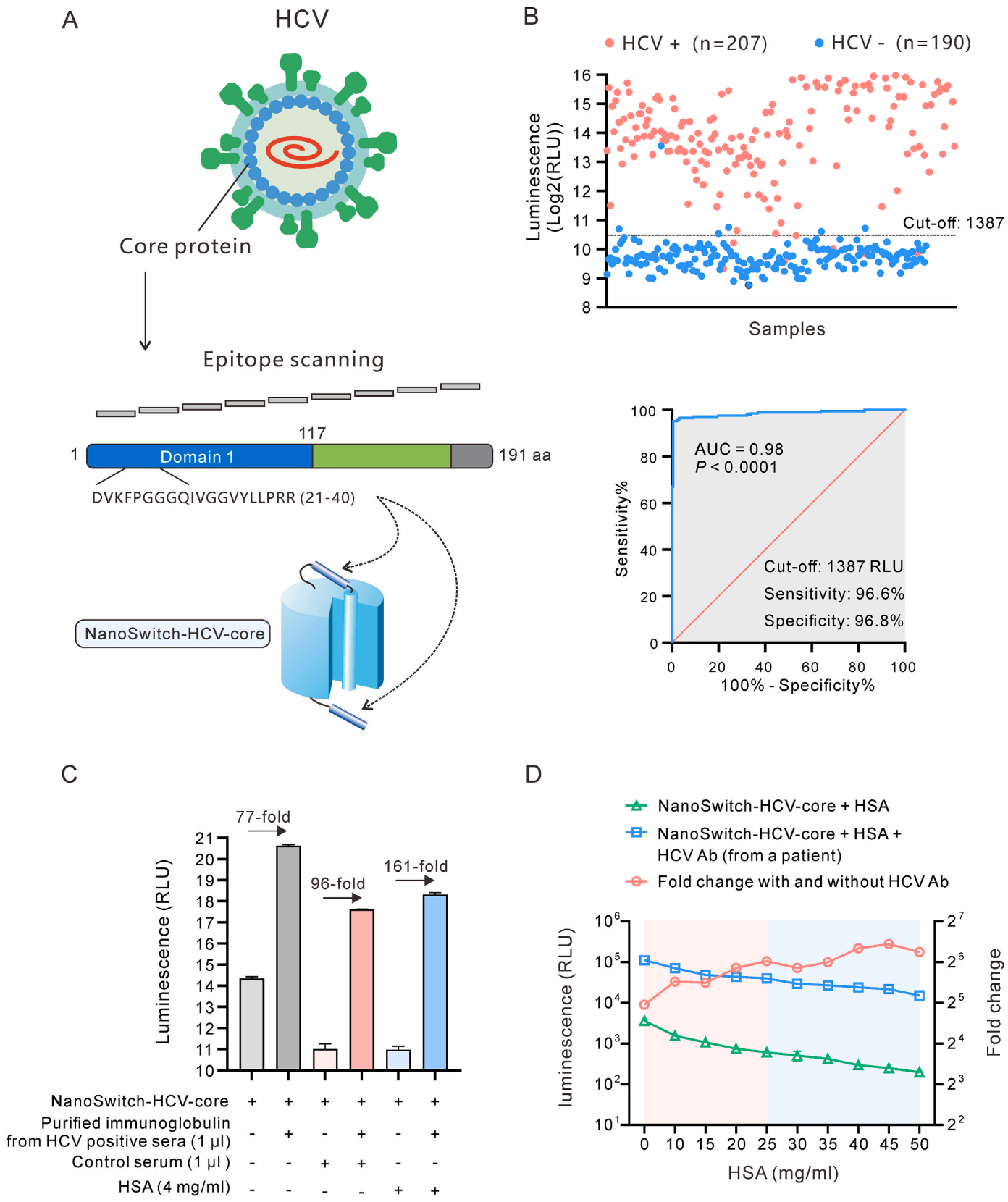

Fig. 4. Development of the NanoSwitch for the detection of HCV antibody
(A) Peptides from the core protein of HCV tested for screening epitopes for the construction of NanoSwitch; **(B)** Assay of HCV-positive and HCV-negative sera by NanoSwitch-HCV-core; **(C)** HSA in serum increased the S/N of the NanoSwitch-HCV-core; **(D)** Responses of NanoSwitch-HCV-core to the purified immunoglobin from the serum sample in the presence of different concentrations of HSA. * Note: Protein reaction buffer (Materials and Methods) was used in Fig. 4 B, C, D, and the reaction was carried out at pH 7.5 and 37 °C.

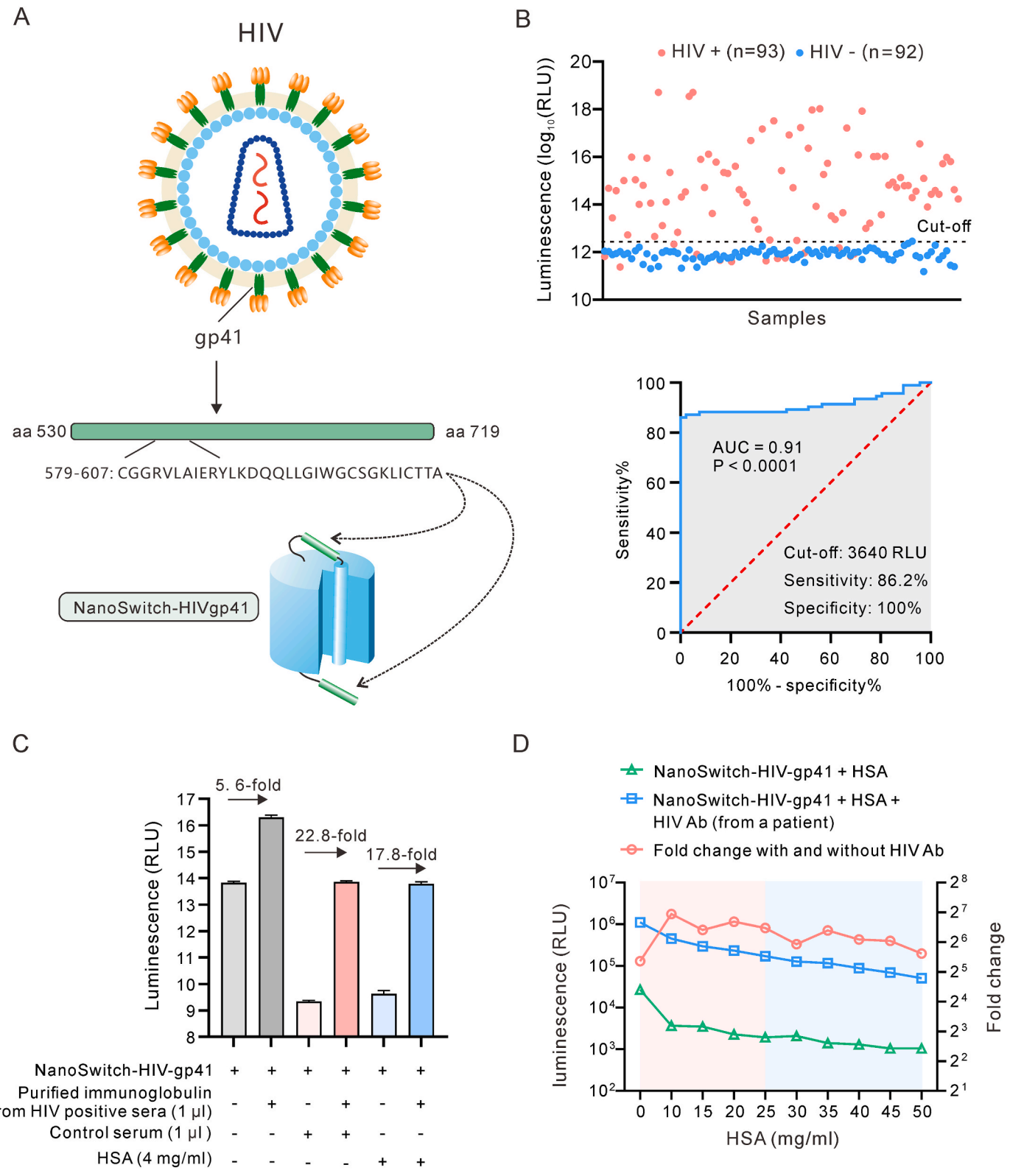

Fig. 5. Development of the NanoSwitch for the detection of HIV antibodies
(A) The peptide from gp41 for the construction of NanoSwitch-HIV-gp41; **(B)** Assay of HIV-positive and HIV-negative sera by NanoSwitch-HIV-gp41; **(C)** HSA in serum increased the S/N of NanoSwitch-HIV-gp41. **(D)** Influence of different concentrations of HSA on the performance of NanoSwitch-HIV-gp41. * Note: Protein reaction buffer (Materials and Methods) was used in Fig. 5 B, C, D, and the reaction was carried out at pH 7.5 and 37 °C.

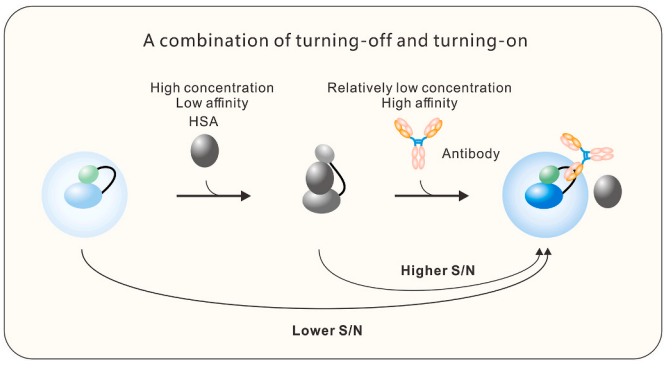

Fig. 6. Nano Switch works in a combination of OFF and ON models to achieve a high S/N.

with a 5.6-fold increase in chemiluminescence (Fig. 5C). Adding 1 μl of control serum in advance augmented the S/N to 22.8-fold; as expected, a similar augmentation in S/N (17.8-fold) was achieved by adding 4 mg/ml HSA to the system. These findings again suggest that NanoSwitch-HIV-gp41 operates in a combination of off-and-on models in the detection of gp41 antibodies in serum samples. In addition, the impact of HSA on the performance of NanoSwitch-HIV-gp41 was tested. The findings showed that HSA had no significant effect on NanoSwitch-HIV-gp41 performance in the range of 25–50 mg/ml (Fig. 5D).

4. Discussion

In the detection of clinical samples, a high S/N of an assay is critical to minimize the effect of background variation of different patients. The S/N of a protein switch based on allosteric enzymes is established by two factors. First, how large is the change in the enzymatic activity after target binding. Secondly, whether the switch operates in a turning-on or turning-off model. Generally, a turning-on protein switch has an advantage over a turning-off switch in S/N because the former harbors a lower background signal. Therefore, a switch that responds to target binding with substantial augmentation in its activity is preferable. One approach to constructing such a switch is using an enzyme suppressor that can be released by binding a target. Switches designed based on this strategy, including LOCKER (Ng et al., 2019; Quijano-Rubio et al., 2021) and sensors exploiting an inhibitor protein of TEM1-β-lactamase (Adamson et al., 2019) perform effectively in some cases. Nonetheless, these switches do not appear satisfactory in the detection of antibodies, with S/Ns less than 10-fold. Also, although we attempted this strategy on NanoLuc using an inhibitor peptide, it was unsuccessful (unpublished data).

The NanoSwitch developed in this study followed an alternative strategy. SmBiT was fused with a linker to the N-terminus of LgBiT, a complementary component of the complete enzyme. The low affinity between SmBiT and LgBiT triggers a state of the enzyme susceptible to the impact induced by events adjacently occurring on the molecule, including the binding of an antibody to the epitope closely placed to SmBiT (Fig. 1A). Noteworthy, the effects of antibody binding can be negative or positive; all the NanoSwitches except NanoSwitch-Flag responded to the binding of the antibody with enhanced activity. Unexpectedly, the binding between SmBiT and LgBiT was easily strengthened rather than disrupted by the attachment of an antibody. Epitopes incorporated into the NanoSwitches might inhibit the interaction between SmBiT and LgBiT, whereas the binding of antibodies released this inhibition. Nevertheless, evidence supporting this hypothesis remains unknown.

Additionally, high S/Ns of a few NanoSwitches, particularly NanoSwitch-PG4-MC are attributed to a previously unreported off-and-on working model (Fig. 6). By careful investigation, we confirmed that HSA in serum is the substance turning off the NanoSwitches. Of note, it is not strange that HSA with a high concentration interacting with numerous molecules binds to NanoSwitches. This binding is partly associated with SmBiT and LgBiT (Fig. 3I) and related to the peptides (epitopes) incorporated because the extent of inhibition is different for different NanoSwitches (Fig. 3I). Our results demonstrate the power of combining turning off and turning on of a switch (Fig. 6). The binding of HSA to NanoSwitch-PG4-MC drastically switched it to the off mode (approximately 40-fold inhibition at 4 mg/ml), providing a preferable baseline for subsequent turning-on by SARS-CoV-2 antibodies. Consequently, SARS-CoV-2 antibodies in serum turned on the switch occupied by HSA by $>$ 200-fold, tremendously higher than the 2-fold increase in signal directly induced by the antibodies (deduced from the data in Fig. 2B). In line with this, multiclonal antibodies against the peptide covering PG4 turned on the HSA-occupied switch by 30-fold. Consistent with these observations, the performance of NanoSwitch-HCV-core and NanoSwitch-HIV-gp41 can be improved by adding HSA (Figs. 4C and 5C). Using the NanoSwitch-PG4-MC, serum samples of COVID-19 patients were precisely discriminated from samples of non-COVID-19 individuals (Fig. 2C and D). More importantly, this switch successfully reported all of the seroconversions, which had been confirmed by a highly sensitive chemiluminescence method based on antibody capture (Fig. 2E and Supplementary Fig. 1). This suggests a robust performance of this method in a real-world application.

In conclusion, we developed a novel type of protein switch for detecting antibodies that can achieve a high S/N using an off-and-on composite working model. Notably, these switches can potentially be applied in the homogeneous analysis of antibodies in clinical settings.

Funding

This work was supported by grants from the National Natural Science Foundation of China (81871635, 81671997, U20A20392, and 81902060), the Natural Science Foundation of Chongqing (cstc2021jcyj-msxmX0298, cstc2020jcyj-msxmX0764 and cstc2020jscx-dxwtBX0022), the Science and Technology Commission of Yuzhong District, Chongqing (20180141), the 111 Project (No. D20028), and Key Laboratory of Molecular Biology on Infectious Diseases, Ministry of Education, Chongqing Medical University (No. 202104).

Data availability

All the data and plasmids are available from the corresponding authors upon request.

CRediT authorship contribution statement

Jie Li: Conceptualization, Methodology, Investigation, Writing – original draft. **Jin-Lan Wang:** Methodology, Investigation. **Wen-Lu Zhang:** Methodology. **Zeng Tu:** Investigation. **Xue-Fei Cai:** Methodology, Investigation. **Yu-Wei Wang:** Investigation. **Chun-Yang Gan:** Methodology. **Hai-Jun Deng:** Investigation. **Jing Cui:** Investigation. **Zhao-Che Shu:** Investigation. **Quan-Xin Long:** Investigation. **Juan Chen:** Resources. **Ni Tang:** Resources. **Xue Hu:** Investigation, Writing – review & editing, Resources, Supervision. **Ai-Long Huang:** Writing – review & editing, Funding acquisition, Resources, Supervision. **Jie-Li Hu:** Conceptualization, Methodology, Investigation, Writing – original draft, Writing – review & editing, Funding acquisition, Supervision.

Declaration of competing interest

The authors declare that they have no known competing financial interests or personal relationships that could have appeared to influence the work reported in this paper.

Acknowledgments

We thank Dr. Bei-Zhong Liu and Gui-Cheng Wu for collecting COVID-19 serum samples.

Appendix A. Supplementary data

Supplementary data to this article can be found online at https://doi.org/10.1016/j.bios.2022.114226.

References

Adamson, H., Ajayi, M.O., Campbell, E., Brachi, E., Tiede, C., Tang, A.A., Adams, T.L., Ford, R., Davidson, A., Johnson, M., McPherson, M.J., Tomlinson, D.C., Jeuken, L.J. C., 2019. Affimer-enzyme-inhibitor switch sensor for rapid wash-free assays of multimeric proteins. ACS Sens. 4, 3014–3022. https://doi.org/10.1021/acssensors.9b01574.

Arts, R., den Hartog, I., Zijlema, S.E., Thijssen, V., van der Beelen, S.H.E., Merkx, M., 2016. Detection of antibodies in blood plasma using bioluminescent sensor proteins and a smartphone. Anal. Chem. 88, 4525–4532. https://doi.org/10.1021/acs.analchem.6b00534.

Arts, R., Ludwig, S.K.J., van Gerven, B.C.B., Estirado, E.M., Milroy, L.-G., Merkx, M., 2017. Semisynthetic bioluminescent sensor proteins for direct detection of antibodies and small molecules in solution. ACS Sens. 2, 1730–1736. https://doi.org/10.1021/acssensors.7b00695.

Azad, T., Tashakor, A., Hosseinkhani, S., 2014. Split-luciferase complementary assay: applications, recent developments, and future perspectives. Anal. Bioanal. Chem. 406, 5541–5560. https://doi.org/10.1007/s00216-014-7980-8.

Banala, S., Aper, S.J.A., Schalk, W., Merkx, M., 2013a. Switchable reporter enzymes based on mutually exclusive domain interactions allow antibody detection directly in solution. ACS Chem. Biol. 8, 2127–2132. https://doi.org/10.1021/cb400406x.

Banala, S., Arts, R., Aper, S.J.A., Merkx, M., 2013b. No washing, less waiting: engineering biomolecular reporters for single-step antibody detection in solution. Org. Biomol. Chem. 11, 7642–7649. https://doi.org/10.1039/c3ob41315b.

Chen, T.-W., Wardill, T.J., Sun, Y., Pulver, S.R., Renninger, S.L., Baohan, A., Schreiter, E. R., Kerr, R.A., Orger, M.B., Jayaraman, V., Looger, L.L., Svoboda, K., Kim, D.S., 2013. Ultrasensitive fluorescent proteins for imaging neuronal activity. Nature 499, 295–300. https://doi.org/10.1038/nature12354.

Dixon, A.S., Schwinn, M.K., Hall, M.P., Zimmerman, K., Otto, P., Lubben, T.H., Butler, B. L., Binkowski, B.F., Machleidt, T., Kirkland, T.A., Wood, M.G., Eggers, C.T., Encell, L. P., Wood, K.V., 2016. NanoLuc complementation reporter optimized for accurate measurement of protein interactions in cells. ACS Chem. Biol. 11, 400–408. https://doi.org/10.1021/acschembio.5b00753.

Elledge, S.K., Zhou, X.X., Byrnes, J.R., Martinko, A.J., Lui, I., Pance, K., Lim, S.A., Glasgow, J.E., Glasgow, A.A., Turcios, K., Iyer, N.S., Torres, L., Peluso, M.J., Henrich, T.J., Wang, T.T., Tato, C.M., Leung, K.K., Greenhouse, B., Wells, J.A., 2021. Engineering luminescent biosensors for point-of-care SARS-CoV-2 antibody detection. Nat. Biotechnol. 39, 928–935. https://doi.org/10.1038/s41587-021-00878-8.

Engler, C., Kandzia, R., Marillonnet, S., 2008. A one pot, one step, precision cloning method with high throughput capability. PLoS One 3, e3647. https://doi.org/10.1371/journal.pone.0003647.

Feliu, J.X., Ferrer-Miralles, N., Blanco, E., Cazorla, D., Sobrino, F., Villaverde, A., 2002. Enhanced response to antibody binding in engineered beta-galactosidase enzymatic sensors. Biochim. Biophys. Acta 1596, 212–224. https://doi.org/10.1016/s0167-4838(02)00226-1.

Ferrer-Miralles, N., Feliu, J.X., Vandevuer, S., Müller, A., Cabrera-Crespo, J., Ortmans, I., Hoffmann, F., Cazorla, D., Rinas, U., Prévost, M., Villaverde, A., 2001. Engineering regulable Escherichia coli beta-galactosidases as biosensors for anti-HIV antibody detection in human sera. J. Biol. Chem. 276, 40087–40095. https://doi.org/10.1074/jbc.M104704200.

Frommer, W.B., Davidson, M.W., Campbell, R.E., 2009. Genetically encoded biosensors based on engineered fluorescent proteins. Chem. Soc. Rev. 38, 2833–2841. https://doi.org/10.1039/b907749a.

Geddie, M.L., Matsumura, I., 2007. Antibody-induced oligomerization and activation of an engineered reporter enzyme. J. Mol. Biol. 369, 1052–1059. https://doi.org/10.1016/j.jmb.2007.03.076.

Griss, R., Schena, A., Reymond, L., Patiny, L., Werner, D., Tinberg, C.E., Baker, D., Johnsson, K., 2014. Bioluminescent sensor proteins for point-of-care therapeutic drug monitoring. Nat. Chem. Biol. 10, 598–603. https://doi.org/10.1038/nchembio.1554.

Guntas, G., Mansell, T.J., Kim, J.R., Ostermeier, M., 2005. Directed evolution of protein switches and their application to the creation of ligand-binding proteins. Proc. Natl. Acad. Sci. U.S.A. 102, 11224–11229. https://doi.org/10.1073/pnas.0502673102.

Guo, Z., Johnston, W.A., Whitfield, J., Walden, P., Cui, Z., Wijker, E., Edwardraja, S., Retamal Lantadilla, I., Ely, F., Vickers, C., Ungerer, J.P.J., Alexandrov, K., 2019. Generalizable protein biosensors based on synthetic switch modules. J. Am. Chem. Soc. 141, 8128–8135. https://doi.org/10.1021/jacs.8b12298.

Hall, M.P., Unch, J., Binkowski, B.F., Valley, M.P., Butler, B.L., Wood, M.G., Otto, P., Zimmerman, K., Vidugiris, G., Machleidt, T., Robers, M.B., Benink, H.A., Eggers, C. T., Slater, M.R., Meisenheimer, P.L., Klaubert, D.H., Fan, F., Encell, L.P., Wood, K.V., 2012. Engineered luciferase reporter from a deep sea shrimp utilizing a novel imidazopyrazinone substrate. ACS Chem. Biol. 7, 1848–1857. https://doi.org/10.1021/cb3002478.

Huston, J.S., Levinson, D., Mudgett-Hunter, M., Tai, M.S., Novotný, J., Margolies, M.N., Ridge, R.J., Bruccoleri, R.E., Haber, E., Crea, R., 1988. Protein engineering of antibody binding sites: recovery of specific activity in an anti-digoxin single-chain Fv analogue produced in Escherichia coli. Proc. Natl. Acad. Sci. U.S.A. 85, 5879–5883. https://doi.org/10.1073/pnas.85.16.5879.

Isazadeh, M., Amandadi, M., Haghdoust, F., Lotfollazadeh, S., Orzáez, M., Hosseinkhani, S., 2022. Split-luciferase complementary assay of NLRP3 PYD-PYD interaction indicates inflammasome formation during inflammation. Anal. Biochem. 638, 114510. https://doi.org/10.1016/j.ab.2021.114510.

Joel, S., Turner, K.B., Daunert, S., 2014. Glucose recognition proteins for glucose sensing at physiological concentrations and temperatures. ACS Chem. Biol. 9, 1595–1602. https://doi.org/10.1021/cb500132g.

Kim, H., Ju, J., Lee, H.N., Chun, H., Seong, J., 2021. Genetically encoded biosensors based on fluorescent proteins. Sensors 21. https://doi.org/10.3390/s21030795.

Legendre, D., Soumillion, P., Fastrez, J., 1999. Engineering a regulatable enzyme for homogeneous immunoassays. Nat. Biotechnol. 17, 67–72. https://doi.org/10.1038/5243.

Long, Q.-X., Liu, B.-Z., Deng, H.-J., Wu, G.-C., Deng, K., Chen, Y.-K., Liao, P., Qiu, J.-F., Lin, Y., Cai, X.-F., Wang, D.-Q., Hu, Y., Ren, J.-H., Tang, N., Xu, Y.-Y., Yu, L.-H., Mo, Z., Gong, F., Zhang, X.-L., Tian, W.-G., Hu, L., Zhang, X.-X., Xiang, J.-L., Du, H.-X., Liu, H.-W., Lang, C.-H., Luo, X.-H., Wu, S.-B., Cui, X.-P., Zhou, Z., Zhu, M.-M., Wang, J., Xue, C.-J., Li, X.-F., Wang, L., Li, Z.-J., Wang, K., Niu, C.-C., Yang, Q.-J., Tang, X.-J., Zhang, Y., Liu, X.-M., Li, J.-J., Zhang, D.-C., Zhang, F., Liu, P., Yuan, J., Li, Q., Hu, J.-L., Chen, J., Huang, A.-L., 2020. Antibody responses to SARS-CoV-2 in patients with COVID-19. Nat. Med. 26, 845–848. https://doi.org/10.1038/s41591-020-0897-1.

Nagai, T., Sawano, A., Park, E.S., Miyawaki, A., 2001. Circularly permuted green fluorescent proteins engineered to sense Ca2+. Proc. Natl. Acad. Sci. U.S.A. 98, 3197–3202. https://doi.org/10.1073/pnas.051636098.

Ng, A.H., Nguyen, T.H., Gómez-Schiavon, M., Dods, G., Langan, R.A., Boyken, S.E., Samson, J.A., Waldburger, L.M., Dueber, J.E., Baker, D., El-Samad, H., 2019. Modular and tunable biological feedback control using a de novo protein switch. Nature 572, 265–269. https://doi.org/10.1038/s41586-019-1425-7.

Ni, Y., Rosier, B.J.H.M., van Aalen, E.A., Hanckmann, E.T.L., Biewenga, L., Pistikou, A.-M.M., Timmermans, B., Vu, C., Roos, S., Arts, R., Li, W., de Greef, T.F.A., van Borren, M.M.G.J., van Kuppeveld, F.J.M., Bosch, B.-J., Merkx, M., 2021. A plug-and-play platform of ratiometric bioluminescent sensors for homogeneous immunoassays. Nat. Commun. 12, 4586. https://doi.org/10.1038/s41467-021-24874-3.

Poh, C.M., Carissimo, G., Wang, B., Amrun, S.N., Lee, C.Y.-P., Chee, R.S.-L., Fong, S.-W., Yeo, N.K.-W., Lee, W.-H., Torres-Ruesta, A., Leo, Y.-S., Chen, M.I.-C., Tan, S.-Y., Chai, L.Y.A., Kalimuddin, S., Kheng, S.S.G., Thien, S.-Y., Young, B.E., Lye, D.C., Hanson, B.J., Wang, C.-I., Renia, L., Ng, L.F.P., 2020. Two linear epitopes on the SARS-CoV-2 spike protein that elicit neutralising antibodies in COVID-19 patients. Nat. Commun. 11, 2806. https://doi.org/10.1038/s41467-020-16638-2.

Quijano-Rubio, A., Yeh, H.-W., Park, J., Lee, H., Langan, R.A., Boyken, S.E., Lajoie, M.J., Cao, L., Chow, C.M., Miranda, M.C., Wi, J., Hong, H.J., Stewart, L., Oh, B.-H., Baker, D., 2021. De novo design of modular and tunable protein biosensors. Nature 591, 482–487. https://doi.org/10.1038/s41586-021-03258-z.

Rabbani, G., Ahn, S.N., 2019. Structure, enzymatic activities, glycation and therapeutic potential of human serum albumin: a natural cargo. Int. J. Biol. Macromol. 123, 979–990. https://doi.org/10.1016/j.ijbiomac.2018.11.053.

Stein, V., Alexandrov, K., 2015. Synthetic protein switches: design principles and applications. Trends Biotechnol. 33, 101–110. https://doi.org/10.1016/j.tibtech.2014.11.010.

Torkzadeh-Mahani, M., Ataei, F., Nikkhah, M., Hosseinkhani, S., 2012. Design and development of a whole-cell luminescent biosensor for detection of early-stage of apoptosis. Biosens. Bioelectron. 38, 362–368. https://doi.org/10.1016/j.bios.2012.06.034.

van Rosmalen, M., Ni, Y., Vervoort, D.F.M., Arts, R., Ludwig, S.K.J., Merkx, M., 2018. Dual-color bioluminescent sensor proteins for therapeutic drug monitoring of antitumor antibodies. Anal. Chem. 90, 3592–3599. https://doi.org/10.1021/acs.analchem.8b00041.

Villaverde, A., 2003. Allosteric enzymes as biosensors for molecular diagnosis. FEBS Lett. 554, 169–172. https://doi.org/10.1016/s0014-5793(03)01160-8.

Weaving, G., Batstone, G.F., Jones, R.G., 2016. Age and sex variation in serum albumin concentration: an observational study. Ann. Clin. Biochem. 53, 106–111. https://doi.org/10.1177/0004563215593561.

Yao, Z., Drecun, L., Aboualizadeh, F., Kim, S.J., Li, Z., Wood, H., Valcourt, E.J., Manguiat, K., Plenderleith, S., Yip, L., Li, X., Zhong, Z., Yue, F.Y., Closas, T., Snider, J., Tomic, J., Drews, S.J., Drebot, M.A., McGeer, A., Ostrowski, M., Mubareka, S., Rini, J.M., Owen, S., Stagljar, I., 2021. A homogeneous split-luciferase assay for rapid and sensitive detection of anti-SARS CoV-2 antibodies. Nat. Commun. 12, 1806. https://doi.org/10.1038/s41467-021-22102-6.

Yu, Q., Pourmandi, N., Xue, L., Gondrand, C., Fabritz, S., Bardy, D., Patiny, L., Katsyuba, E., Auwerx, J., Johnsson, K., 2019. A biosensor for measuring NAD(+) levels at the point of care. Nat. Metab. 1, 1219–1225. https://doi.org/10.1038/s42255-019-0151-7.

Yu, Q., Xue, L., Hiblot, J., Griss, R., Fabritz, S., Roux, C., Binz, P.-A., Haas, D., Okun, J.G., Johnsson, K., 2018. Semisynthetic sensor proteins enable metabolic assays at the point of care. Science 361, 1122–1126. https://doi.org/10.1126/science.aat7992.